Ectodermal *Wnt3*/β-*catenin* signaling is required for the establishment and maintenance of the apical ectodermal ridge

Jeffery R. Barrow,[1] Kirk R. Thomas,[2] Oreda Boussadia-Zahui,[3,4] Robert Moore,[3,5] Rolf Kemler,[3] Mario R. Capecchi,[2] and Andrew P. McMahon[1,6]

[1]Department of Molecular and Cellular Biology, Harvard University, Cambridge, Massachusetts 02138, USA; [2]Howard Hughes Medical Institute, Department of Human Genetics, University of Utah School of Medicine, Salt Lake City, Utah 84112, USA; [3]Department of Molecular Embryology, Max-Planck Institute of Immunobiology, D-79108 Freiberg, Germany.

The formation of the apical ectodermal ridge (AER) is critical for the distal outgrowth and patterning of the vertebrate limb. Recent work in the chick has demonstrated that interplay between the *Wnt* and *Fgf* signaling pathways is essential in the limb mesenchyme and ectoderm in the establishment and perhaps the maintenance of the AER. In the mouse, whereas a role for *Fgfs* for AER establishment and function has been clearly demonstrated, the role of *Wnt*/β-*catenin* signaling, although known to be important, is obscure. In this study, we demonstrate that *Wnt3*, which is expressed ubiquitously throughout the limb ectoderm, is essential for normal limb development and plays a critical role in the establishment of the AER. We also show that the conditional removal of β-*catenin* in the ventral ectodermal cells is sufficient to elicit the mutant limb phenotype. In addition, removing β-*catenin* after the induction of the ridge results in the disappearance of the AER, demonstrating the requirement for continued β-*catenin* signaling for the maintenance of this structure. Finally, we demonstrate that *Wnt*/β-*catenin* signaling lies upstream of the *Bmp* signaling pathway in establishment of the AER and regulation of the dorsoventral polarity of the limb.

[*Keywords*: Limb; *Wnt*/β-*catenin* signaling; apical ectodermal ridge; mouse]

Supplemental material is available at http://www.genesdev.org.

Received September 25, 2002; revised version accepted December 6, 2002.

The formation of the apical ectodermal ridge (AER) has long been known to play a critical role in the distal outgrowth and patterning of the vertebrate limb. Classical experiments performed by Saunders (1948) demonstrated that surgical removal of this tissue shortly after its formation results in severe truncations of the entire limb, whereas removal at progressively later stages in development allows outgrowth of the more distal elements in a progressive fashion. Given the critical role that the AER plays in limb development, a major focus within the limb field has been to identify molecules that are involved in its establishment and maintenance. The result of this effort has been the discovery that several signaling pathways interact in the establishment of the AER. For example, recent work in the chick has demonstrated that cooperation between the *Wnt*/β-*catenin* and *Fgf* signaling pathways is essential in establishing the AER. Briefly, the prevailing model is as follows: *Wnt*/β-*catenin* signaling in the limb mesenchyme appears to be required to activate *Fgf10* expression in the same tissue (Kawakami et al. 2001). Mesenchymally derived *Fgf10* then regulates expression of *Wnt3a* in the overlying surface ectoderm and later in the subset of ectodermal cells that is destined to give rise to the AER (Kengaku et al. 1997, 1998). *Wnt3a* signaling is then thought to act through the β-catenin pathway to activate the expression of *Fgf8* in these pre-AER cells (Kengaku et al. 1998). *Fgf8* signaling to the mesenchyme maintains *Fgf10* expression, presumably through the mesenchymal *Wnt*/β-*catenin* pathway, thereby completing a regulatory circuit that is critical for maintenance of the AER (see Kawakami et al. 2001).

In the mouse, genetic evidence supports the involvement of both *Fgf* and *Wnt*/β-*catenin* signaling in forma-

Present addresses: [4]Nucleis, Parc technologique des capucins, Bâtiment Montéclair, F-49033 Angers, cedex 01, France; [5]Génétique du Développement des Mélanocytes, Institut Curie, F-91405 Orsay, France.
[6]Corresponding author.
E-MAIL amcmahon@mcb.harvard.edu; FAX (617) 496-3763.
Article and publication are at http://www.genesdev.org/cgi/doi/10.1101/gad.1044903.

tion of the AER. For example, loss of Fgf10, or of other molecules that act downstream to transduce Fgf10 signaling, abolishes formation of the AER (Min et al. 1998; Sekine et al. 1999; Saxton et al. 2000). Further, additional AER-derived *Fgf* signals, *Fgf4* and *Fgf8*, are required for AER function, though not for AER formation (Lewandoski et al. 2000; Moon and Capecchi 2000; Sun et al. 2002).

Although the roles of *Fgfs* in the limb ectoderm and mesenchyme in the mouse are beginning to be elucidated, those of the *Wnt*/β-*catenin* pathway remain obscure. Mouse embryos lacking the *Wnt*/β-*catenin* pathway components, *LRP6* or simultaneously *Lef1* and *Tcf1*, exhibit defects in the formation of the AER, demonstrating that this pathway is indeed required for AER formation (Galceran et al. 1999; Pinson et al. 2000). However, because these components are ubiquitously expressed in the limb mesenchyme and ectoderm, it is not yet clear whether it is the mesenchymal or ectodermal requirement of *Wnt*/β-*catenin* signaling (or both) that has been disrupted in these mutants, nor is it clear which *Wnt* ligands regulate the β-*catenin* pathway in these tissues. In the chick, *Wnt3a* is expressed at the right time and place in the limb ectoderm to mediate the *Wnt*/β-*catenin* signaling required for establishment of the AER. In the mouse, however, *Wnt3a* is not expressed in the limb ectoderm (Roelink and Nusse 1991; Takada et al. 1994), and mouse embryos lacking Wnt3a activity do not exhibit limb defects (Takada et al. 1994). In contrast, a closely related family member, *Wnt3*, is expressed in the limb ectoderm (Roelink and Nusse 1991); however, the early lethality of *Wnt3* mutants has precluded analysis of its role in limb development (Liu et al. 1999; W. Howell and M.R. Capecchi, unpubl.).

In addition to the *Wnt*/β-*catenin* and *Fgf* signaling pathways, *Bmp* signaling has also been demonstrated to play an important role in establishing dorsoventral patterning in the limb ectoderm (Ahn et al. 2001; Pizette et al. 2001), a critical step in the establishment and placement of the AER in both the mouse and the chick (for review, see Chen and Johnson 1999). Although the *Bmp* receptor BMP1R is expressed ubiquitously in the limb ectoderm, the restriction of the Bmp ligands, *Bmp2*, *Bmp4*, and *Bmp7* to the ventral ectoderm is necessary to limit signaling to this tissue (Ahn et al. 2001; Pizette et al. 2001). Like the *Wnt*/β-*catenin* and *Fgf* signaling pathways, *Bmp* signaling is also essential for the establishment of the AER. However, it is not clear how these pathways may interact to form this specialized epithelium.

In this study, we demonstrate that *Wnt3* signaling in the limb ectoderm is indeed required for the formation of the AER. We also show, through conditional removal of β-*catenin* in the limb ectoderm, that the pre-AER ventral ectoderm is the critical target of this *Wnt3* signal. Finally, we demonstrate that expression of ventral ectodermal *Bmps* and *Fgf8* in the AER are dependent on *Wnt*/β-*catenin* signaling. Our results provide compelling evidence for an ectodermally active *Wnt3*/β-*catenin* pathway which is essential for formation and maintenance of the AER and consequently outgrowth of the mammalian limb.

Results

Wnt3 *is expressed ubiquitously in the ectoderm*

Several *Wnt* genes are known to be expressed in the mouse and chick limb ectoderm (Martin 1998; A. McMahon and C. Tabin, unpubl.). We re-examined the expression pattern of one of these, *Wnt3*, previously reported to be expressed in the mouse limb ectoderm (Roelink and Nusse 1991). At embryonic day 9.5 (E9.5), we identified *Wnt3* mRNA ubiquitously in the ectoderm of the forelimb bud (Fig. 1A) and at low levels throughout the tail ectoderm, including cells overlying the future hindlimb bud (Fig. 1B, arrowheads). Broad ectodermal expression is maintained in all outgrowing limbs and in ectoderm flanking the limbs until at least through E11.5 (Fig. 1C,D; data not shown).

Conditional removal of Wnt3 *in the limb ectoderm results in severe limb defects*

Mice homozygous for null alleles of *Wnt3* fail to gastrulate and thus never develop limbs (Liu et al. 1999; $Wnt3^{n/n}$ homozygotes: B. Howell and M. Capecchi, unpubl.). To examine the role of *Wnt3* in the limb ectoderm, we therefore undertook a conditional mutagenic approach using Cre/lox*P* recombination to remove the *Wnt3* gene in a tissue-specific fashion. Lox*P* sites flanking exons 3 and 4 (Supplementary Fig. 1D; Materials and Methods) were targeted to the *Wnt3* locus to generate a *Wnt3* conditional allele ($Wnt3^{c}$). To elicit tissue-specific removal of *Wnt3* in the ectoderm of the forelimb, we used a *Cre* transgene under control of the RARβ promoter (*RARCre*); this promoter is active in the forelimb ectoderm prior to formation of the AER but is not active in the hindlimb (Moon and Capecchi 2000; Moon et al. 2000). In addition, we made use of an *Msx2Cre* transgene which has been reported to drive Cre activity in the hindlimb ectoderm prior to formation of the AER and in the AER of the forelimb, after its formation (Sun et al. 2000).

We intercrossed mice to generate $Wnt3^{n/c}$; *RARCre* or $Wnt3^{n/c}$; *Msx2Cre* mutants (see Materials and Methods). Consistent with the previously reported pattern of Cre activity, we found that $Wnt3^{n/c}$; *RARCre* mutant mice exhibited defects only in the forelimb. Although completely penetrant, the severity of the forelimb phenotype was variable, ranging from three digits and a normal zeugopod (Fig. 1F) to forelimbs with a single digit (either digit 2 or 3) and no ulna (Fig. 1G). $Wnt3^{n/c}$; *Msx2Cre* mutant mice exhibited normal forelimbs except in two cases (2/44) where digit 5 was missing or was fused to digit 4 (data not shown). The penetrance and expressivity of the hindlimb phenotype was quite variable; some mice were completely normal (2/44; see Fig. 1H, right hindlimb; Fig. 1K), whereas limbs were entirely absent in others (3/44; Fig. 1O, arrowhead). Most often the pheno-

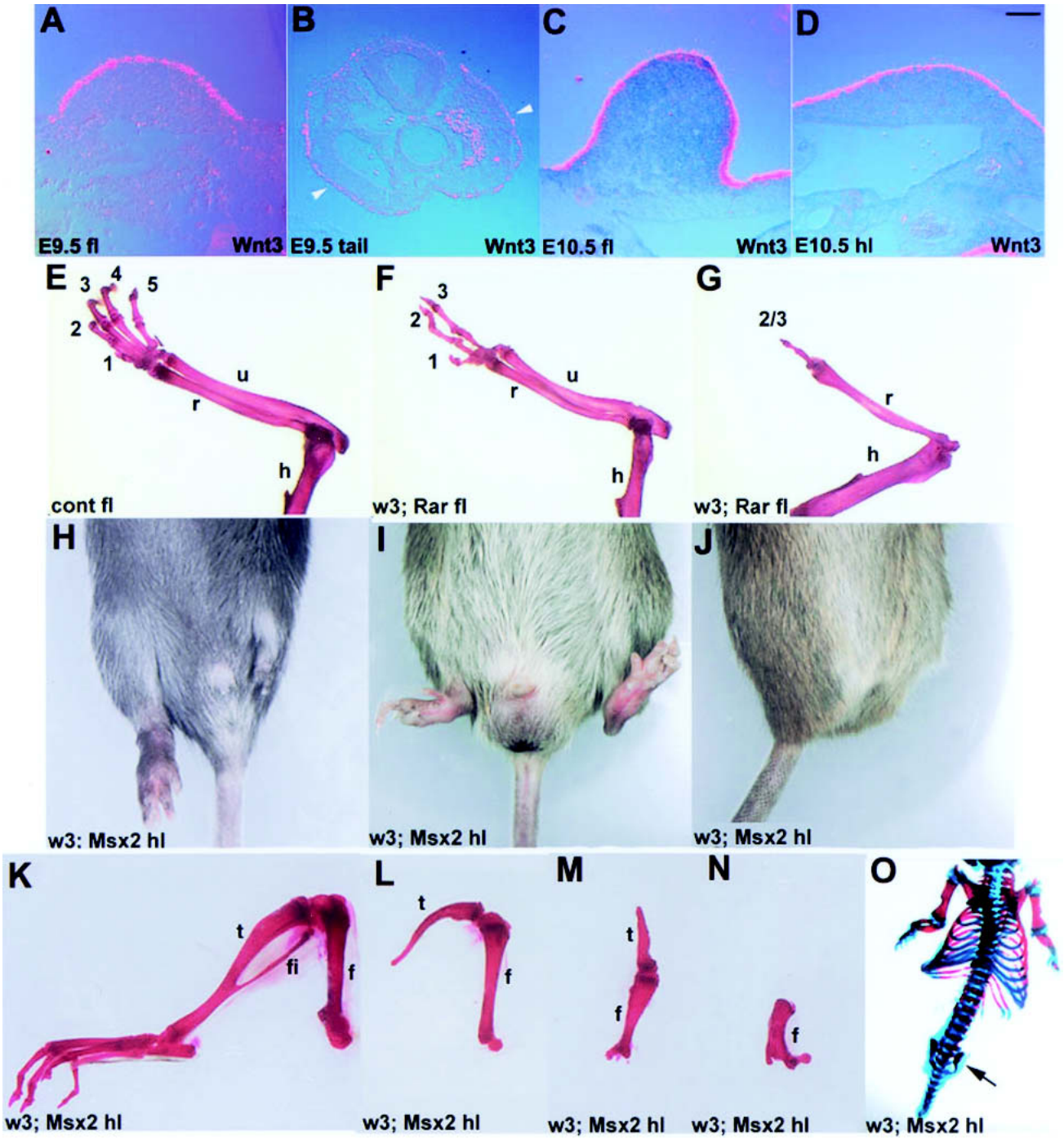

Figure 1. *Wnt3* expression and consequences of its removal in the limb ectoderm. (*A*) *Wnt3* is expressed ubiquitously in the forelimb ectoderm at E9.5. (*B*) Transverse section through the tail at the level of the prospective hindlimbs at E9.5. *Wnt3* is expressed at low levels throughout the ectoderm, including that overlying the prospective limb mesenchyme (arrowheads). (*C*,*D*) *Wnt3* is expressed strongly throughout the ectoderm of both the fore- and hindlimbs at E10.5. (*E–O*) Limb defects in *Wnt3* conditional mutants. (*E–G*) $Wnt3^{n/c}$; *RARCre* mutants exhibit variable forelimb defects ranging from three digits (anterior digits 1–3) and normal zeugopod [radius (r) and ulna (u) in *F*] to one digit (digit 2 or 3) and also zeugopod defects (missing ulna in *G*). The humerus (h) in most instances was unaffected. (*H–O*) The phenotype of $Wnt3^{n/c}$; *Msx2Cre* conditional mutants varied dramatically, ranging from completely normal (*H*, right hindlimb; *K*) to entirely absent (arrow, *O*). cont, control animals; fl, forelimb; h, humerus; hl, hindlimb; numbers (i.e., 1–5) indicate digit number; r, radius; u, ulna; w3; Msx2, $Wnt3^{n/c}$; *Msx2Cre* mutants; w3; Rar, $Wnt3^{n/c}$; *RARCre* mutants; Bar: *A–D*, 100 µm.

type was somewhere between these two extremes, with mice exhibiting mild to severe autopod defects (22/44, Fig. 1I), or more extensive truncations that extended into more proximal segments of the limb (17/44, Fig. 1I,L–O).

Removal of Wnt3 *in the limb ectoderm disrupts formation of the AER*

As the limbs of the *Wnt3* conditional mutants exhibited distal truncations similar to chick limbs in AER extirpation studies, we sought to examine the molecular and morphological consequences of *Wnt3* removal on the formation of the AER. *Fgf8* is an excellent marker for this process, as *Fgf8* is first expressed in cells of the ventral ectoderm that later form the AER; expression then continues within the AER itself until the AER regresses at ~E12.5 (Crossley and Martin 1995). *Fgf8* was not expressed in the anterior or posterior distal margin of the AER but was generally restricted to the central region in the forelimbs of $Wnt3^{n/c}$; *RARCre* embryos at E10.5 (Fig. 2B,C, arrowheads). The absence of anterior and posterior AER correlates with the lack of anterior and posterior digits in these mutants. The $Wnt3^{n/c}$; *Msx2Cre* mutants exhibited variable *Fgf8* expression in the distal margin of the hindlimb consistent with the variation in the skeletal phenotype of the mutants. Thus, at one extreme, we observed *Fgf8* expression throughout the anteroposterior (AP) axis of the distal limb ectoderm (Fig. 2E,H); however, the dorsoventral (DV) girth of the *Fgf8*-stained region was always much thinner than in control embryos. In other cases, we found that *Fgf8* expression was nonexistent or restricted to small patches along the AP axis (Fig. 2F,I; data not shown). The DV girth of the forelimb AER was also reduced; however, the AP length of the AER was generally not disrupted (data not shown). Histological sections of these stained limb buds showed that in controls the *Fgf8*-positive cells corresponded to the thickened ectoderm of the pre-AER or AER, whereas in mutants the expression was restricted to ectoderm that was only slightly thickened or not thickened at all (data not shown). Regions of ectoderm devoid of staining exhibited no thickening (data not shown). Additional sections of $Wnt3^{n/c}$; *Msx2Cre* mutant hindlimbs in other contexts also demonstrated the lack of thickened ectoderm (e.g., Fig. 8E; data not shown). Thus, Wnt3 signaling is critical for the formation of the thickened ectoderm of the AER.

Re-examination of RARCre *and* Msx2Cre *activity in the limb ectoderm*

We next wanted to understand the basis for the variation of the limb defects in *Wnt3* conditional mutants. Although *RARCre* and *Msx2Cre* have been shown to mediate complete removal of genes expressed within the

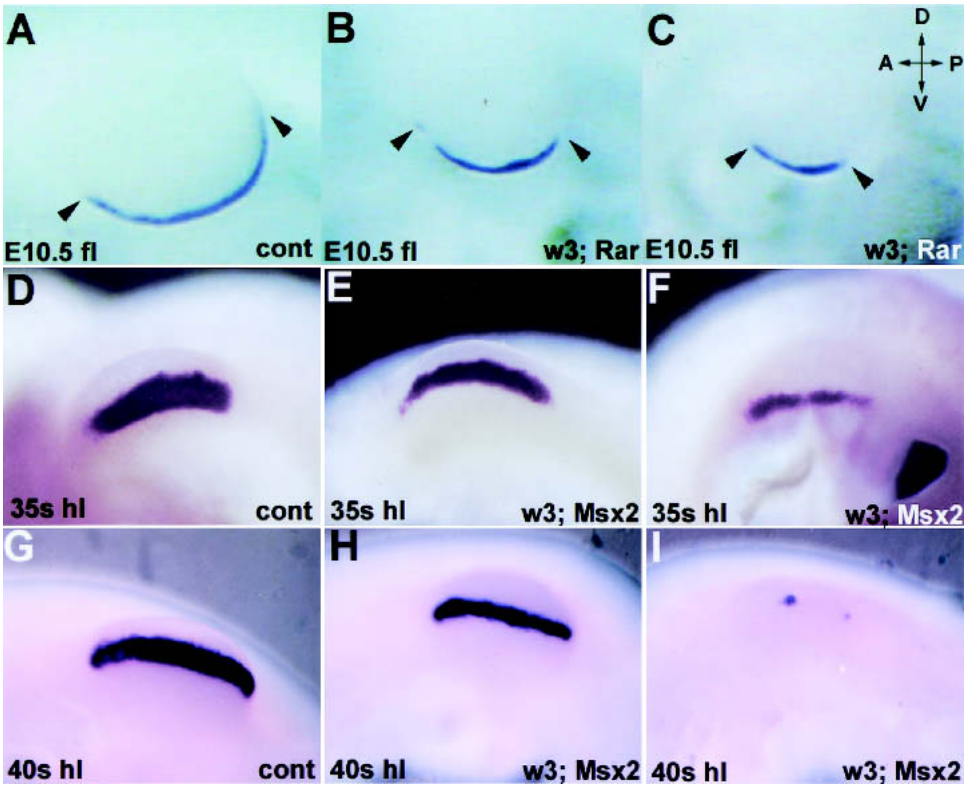

Figure 2. *Fgf8* expression and AER formation are disrupted in *Wnt3* conditional mutants. For *A–I*, dorsal (D) is up, ventral is down, anterior (A) is left, and posterior (P) is right. (*A–C*) $Wnt3^{n/c}$; *RARCre* conditional mutants exhibit a reduction in the anterior/posterior length of the AER (arrowheads). *Fgf8* expression in the *RARCre* mutant hindlimbs is normal. (*D–I*) $Wnt3^{n/c}$; *Msx2Cre* conditional mutants exhibit variability in the expression of *Fgf8*. *E* and *H* represent mutants where *Fgf8* expression has been mildly affected, however, the dorsoventral girth of the AER is reduced to ~50%. *F* and *I* represent variations of severely affected limbs such that *Fgf8* expression is dramatically reduced. cont, control; fl, forelimb; hl, hindlimb; w3; Rar, $Wnt3^{n/c}$; *RARCre*, w3; Msx, $Wnt3^{n/c}$; *Msx2Cre*. Bar, 300 μm.

AER of the fore- and hindlimb, respectively (Lewandoski et al. 2000; Moon and Capecchi 2000; Moon et al. 2000; Sun et al. 2000), we reasoned that because *Wnt3* is expressed ubiquitously in the limb ectoderm, a variability in Cre activity outside the AER could be responsible for a variability in expressivity of the mutant phenotype. We decided therefore to reinvestigate the activity of the *RARCre* and *Msx2Cre* transgenic lines in more detail, using the ROSA26 reporter strain R26R, which activates the expression of *lacZ* upon Cre-mediated recombination (Soriano 1999). At early E9.5, we observed *RARCre* activity throughout the mesenchyme and overlying ectoderm of the forelimb (Fig. 3A–C). At the anterior and posterior extremes (Fig. 3A,C, respectively), Cre activity was ubiquitous throughout the dorsal and ventral ectoderm (Fig. 3, arrowheads denote ventral ectoderm), whereas at more central locations (Fig. 3B) removal was not complete in the dorsal ectoderm. Interestingly, it is in regions where *RARCre* is active in both the dorsal and ventral ectoderm (i.e., the anterior and posterior extremes) where AER formation was disrupted in the $Wnt3^{n/c}$; *RARCre* mutants. In the hindlimb, there was little or no Cre activity in the ectoderm (Fig. 3D), corresponding to the lack of hindlimb defects in the $Wnt3^{n/c}$; *RARCre* mutants. In the case of the *Msx2Cre* transgene, we found important temporal and spatial differences in Cre activity between the fore- and hindlimb. Temporally, we observed strong *Msx2Cre* activity in the hindlimb ectoderm at 19 somites (19s; Fig. 3I), approximately 12 h prior to the induction of the AER as judged by the

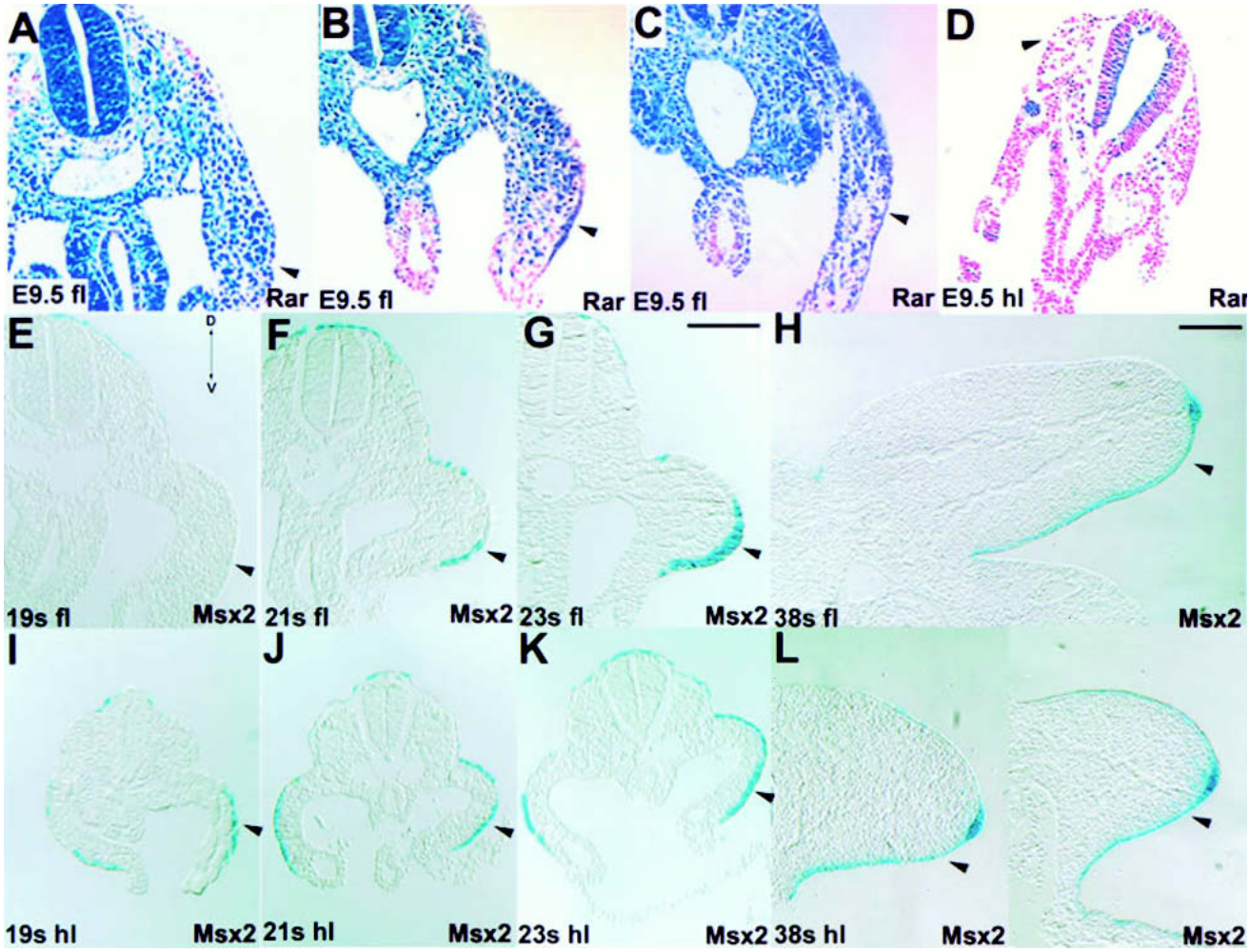

Figure 3. *RARCre* and *Msx2Cre* reporter activity in the limb ectoderm. For all panels ventral is down; accordingly, the arrowhead denotes the ventral ectoderm. (*A–D*) ROSA26 reporter activity for *RARCre* transgenic fore- and hindlimbs. Sections through the anterior (*A*), central (*B*), and posterior (*C*) regions of the forelimb bud. Note the strong Cre activity throughout the ectoderm of the anterior (*A*) and posterior (*C*) sections, whereas the central section (*B*) only exhibits strong activity in the ventral ectoderm (arrowhead). (*D*) Transverse section through the hindlimb. (*E–L*) ROSA26 reporter analysis of *Msx2Cre* transgenic fore- and hindlimbs. (*E*) At 19 somites (19s), Cre activity has not yet commenced in the forelimb ectoderm. (*F*) Cre is active weakly in the ventral ectoderm of 21s transgenic animals (arrowhead). (*G*,*H*) Cre activity is robust throughout the ventral ectoderm and AER. (*I*,*L*) *Msx2Cre* transgenic animals exhibit strong Cre activity throughout the ventral ectoderm of the hindlimbs (arrowheads). There is variable activity in the dorsal ectoderm. 19s, 19 somites; 20s, 20 somites; etc.; D, dorsal; fl, forelimb; hl, hindlimb; Msx2, *Msx2Cre*/R26R double transgenic animals; Rar, *RARCre*/R26R double transgenic embryos; V, ventral. Bars, 100 µm. Bar in *G* is for *E–G*, and *I–K*; bar in *H* is for *H* and *L*.

onset of *Fgf8* expression. In contrast, we did not observe any Cre activity in the forelimb ectoderm until 21 somites (Fig. 3E,F), ~4 h after initiation of *Fgf8* expression in pre-AER cells. Hence, *Msx2Cre* drives strong Cre activity in the hindlimb ectoderm long before the appearance of the AER but only becomes active in the forelimb after induction of AER precursors has commenced. Spatially, Cre activity in the forelimb was restricted to the ventral ectoderm, the AER, and a few cells of the proximal dorsal ectoderm (Fig. 3F–H). In the hindlimb, although we detected ubiquitous Cre activity in the ventral ectoderm and AER similar to the forelimb, variable dorsal ectodermal activity was also observed (Fig. 3J,K, left hindlimb buds) such that in some embryos Cre activity extended into much of the dorsal ectoderm (Fig. 3J,K, right hindlimb buds). Additional variability in the dorsal extent of Cre activity was also observed at different positions along the AP axis of an individual limb bud (Fig. 3L). As with the *Wnt3*$^{n/c}$; *RARCre* forelimbs, we suggest that the AER defects in the *Wnt3*; *Msx2Cre* mutants similarly occur only in regions of the limb where there is both dorsal and ventral *Msx2Cre* activity. Thus, in the hindlimb, where there is ubiquitous ventral Cre activity and variable extents in the dorsal ectoderm, there are correspondingly variable AER defects. In contrast, in the forelimb, where there is only ventral ectodermal Cre activity, there are no AER defects. It could be argued that the lack of AER defects in the forelimb might be due to the late onset of Cre activity in the forelimb, that is, *Wnt3*, although required for the induction of the AER, may only play a redundant role in AER maintenance. However, the *Wnt3*$^{n/c}$; *Msx2Cre* hindlimbs and *Wnt3*$^{n/c}$; *RARCre* forelimbs clearly demonstrate that ventral ectodermal Cre activity is not sufficient to disrupt formation of the AER. We suggest a model where despite ubiquitous *Wnt3* expression in the limb ectoderm, the AER (or pre-AER) may be the only tissue capable of responding to this signal. However, as *Wnt3* is a secreted molecule and likely functions in a cell-nonautonomous fashion, it may be necessary to remove *Wnt3* activity from both the AER and adjacent dorsal and ventral ectoderm to abolish signaling in the AER.

Removal of β-catenin *in the limb ectoderm results in severe limb defects*

β-*catenin* is critical for transducing canonical *Wnt* signals to the nucleus of responding cells, where it participates with *Lef*/*Tcf* transcription factors in the activation of downstream target genes (Behrens et al. 1996; Molenaar et al. 1996). To address *Wnt* responsiveness in the ectoderm of the limb, we undertook an approach where we used β-*catenin* null and conditional alleles (Haegel et al. 1995; Brault et al. 2001) as well as the *Msx2Cre* transgene to specifically remove β-*catenin* from the limb ventral ectoderm of mouse embryos. The AER arises from ventral ectodermal cells which are later restricted to the dorsoventral midline (Bell et al. 1998; Loomis et al. 1998). β-*catenin*$^{n/c}$; *Msx2Cre* mutant mice were born but never nursed and died within 24 h. The cause of death is unknown but presumably reflects *Msx2Cre*-mediated removal of β-*catenin* in tissues outside of the limb. All pups completely lacked hindlimbs; in contrast, forelimbs were present but truncated at the level of the humerus or ulna (Fig. 4A–H).

β-catenin; Msx2Cre *conditional mutants exhibit severe defects in formation and maintenance of the AER*

The absence of hindlimbs and the distal truncations of the forelimbs of β-*catenin; Msx2Cre* pups were consistent with defective AER function. We therefore examined the expression of *Fgf8* in mutant embryonic limbs. In the hindlimb, *Fgf8* was not expressed at any of the stages examined from its onset at 28 somites until at least 38 somites (Fig. 5A–F). In contrast, *Fgf8* expression initiated properly in the forelimb at 20 somites, but subsequently expression became patchy distally and finally disappeared in the anterior and posterior extremes by ~38 somites. Thus, it would appear that AER formation failed to initiate in the hindlimb whereas in the forelimbs, the AER initiated but was not maintained. The basis for this defect likely reflects a temporal difference in the onset of Cre activity in the limb field (see earlier discussion; Fig. 3E–L). Thus β-*catenin* is required for both initiation and maintenance of the AER. Based on two observations, these data also suggest that the dorsal ectoderm is not required to respond to a *Wnt* signal. First, in the forelimb, where no dorsal Cre activity was observed, the AER disappeared after β-*catenin* signaling was removed from the ventral ectoderm. Secondly, the absence of the hindlimb is completely penetrant, which suggests that the hindlimb phenotype is insensitive to variability in dorsal Cre activity. Together the results suggest that reception of the Wnt3 signal in ventral ectoderm may be sufficient to both induce and maintain the AER.

Lack of β-catenin *in the limb ectoderm does not affect cell adhesion or initiation of* Fgf10 *expression in the limb mesenchyme*

In addition to transducing *Wnt* signals to the nucleus, β-catenin plays an important role in E-cadherin-mediated cell adhesion (Aberle et al. 1996). Thus, removal of β-catenin activity in the limb ectoderm might preclude AER formation by disrupting cell adhesion. To address this issue, we examined the localization of E-cadherin in control and β-*catenin*$^{n/c}$; *Msx2Cre* mutant limb buds at 35 somites (Fig. 6) and at E11.5 (data not shown). E-cadherin was appropriately localized at the cell membrane in the ventral ectoderm of the fore- and hindlimbs (Fig. 6B,D,F,H) despite the lack of β-catenin in neighboring sections (Fig. 6A,C,E,G). Thus, the failure of AER formation most likely results from deficits in *Wnt* signaling rather than cell adhesion.

A second critical question is whether ectodermal *Wnt* signaling is downstream of the activation of *Fgf10* expression in the limb mesenchyme as it is in the chick (Kawakami et al. 2001). In β-*catenin*$^{n/c}$; *Msx2Cre* mutant

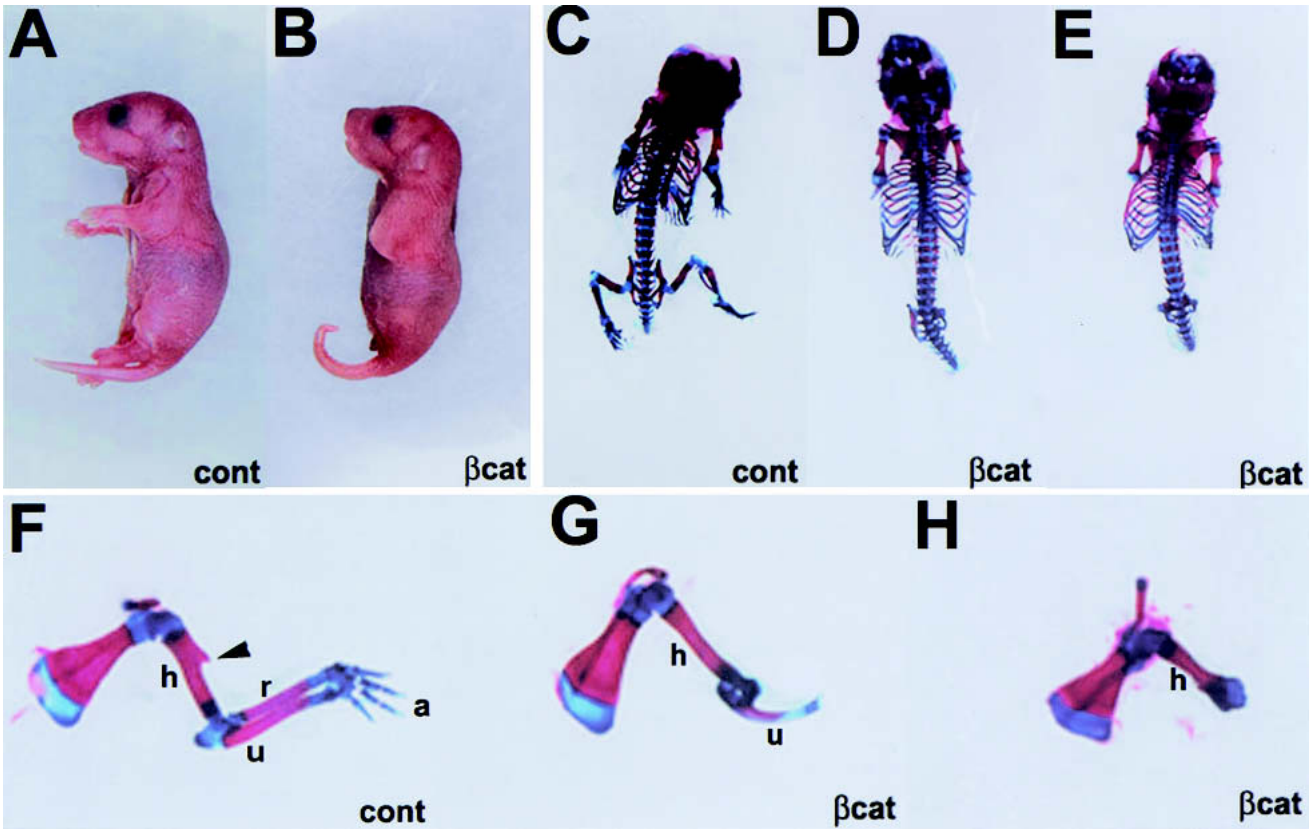

Figure 4. Limb defects in β-*catenin*$^{n/c}$; *Msx2Cre* conditional mutant embryos. Control and mutant newborns (*A*,*B*) and newborn skeletons (*C*–*H*). Note the complete absence of hindlimbs (*B*,*D*,*E*) and that the forelimbs are truncated at the end of the humerus (h; *G*,*H*). The proximal ulna (u) is present to variable extents (*G*,*H*), whereas the humerus is largely unaffected with the exception that the deltoid crest (arrowhead) is absent. a, autopod; βcat, β-*catenin*$^{n/c}$; *Msx2Cre*; cont, control animals, r, radius; u, ulna.

mice, *Fgf10* expression was indistinguishable from control embryos at early hindlimb stages (26 somites; Fig. 6I,J) but expression was not maintained (Fig. 6K,L) Thus, ectodermal *Wnt*/β-*catenin* signaling is required after activation of *Fgf10* expression in the limb mesenchyme for the maintenance of *Fgf10* expression in these cells.

Lack of Wnt/β-catenin *signaling in the limb ectoderm disrupts dorsoventral patterning of the limb*

Establishment of correct DV polarity in the ectoderm of the chick limb bud is important for both the formation and placement of the AER (for review, see Chen and Johnson 1999). Recent work in both the chick and mouse has demonstrated that BMP signaling plays a critical role in this process (Ahn et al. 2001; Pizette et al. 2001). To determine whether *Wnt*/β-*catenin* signaling may play a role in initiating BMP signaling in the early limb ectoderm, we examined the expression of *Bmp2* and *Bmp4*, which are normally expressed in the ventral ectoderm and AER of the mouse limb (Lyons et al. 1990; Ahn et al. 2001). Although in wild-type limbs *Bmp2* and *Bmp4* were both expressed in the ventral ectoderm of 26-somite embryos, we found no evidence of expression of either gene at this or later stages in the hindlimbs of β-*catenin*$^{n/c}$/*Msx2Cre* mutant embryos (Fig. 7A–D; data not shown). A similar disruption in *Bmp2* and *Bmp4* expression was also observed in *Wnt3*-deficient embryos (data not shown). Thus, Wnt3/β-catenin activity appears to lie upstream of *Bmp* factors in the pathways that establish a functional AER.

To further test this relationship, we expressed a dominant active form of β-*catenin* (daβ-*catenin*) in the limb ectoderm of stage 12 chick embryos. At stage 22–24, daβ-*catenin* induced the expression of *Bmp2*, *Bmp4*, and *Bmp7* (Fig. 7F,G,H, respectively) in both the dorsal and ventral ectoderm. However, induction of *Bmp* expression was only observed in 20% (8/46) of infected limbs, whereas induction of *Fgf8* was observed in 95% (15/16; Fig. 7E) of the embryos, indicating that ectopic *Bmp* activity is not essential for induction of *Fgf8* (see below). Further, *Bmp* expression was more restricted, localizing to the thickened ectoderm of the endogenous or ectopic AER.

Additional consequences of deficiencies in dorsoventral patterning in the conditional mutants could be seen in an examination of the expression patterns of *Lmx1b* and *En1*, which are markers for dorsal and ventral fates of the limb, respectively. The β-*catenin* mutant hindlimbs exhibited a complete absence of *En1* expression in the ventral ectoderm, whereas *Lmx1b* expression, which is typically restricted to the dorsal mesenchyme, was

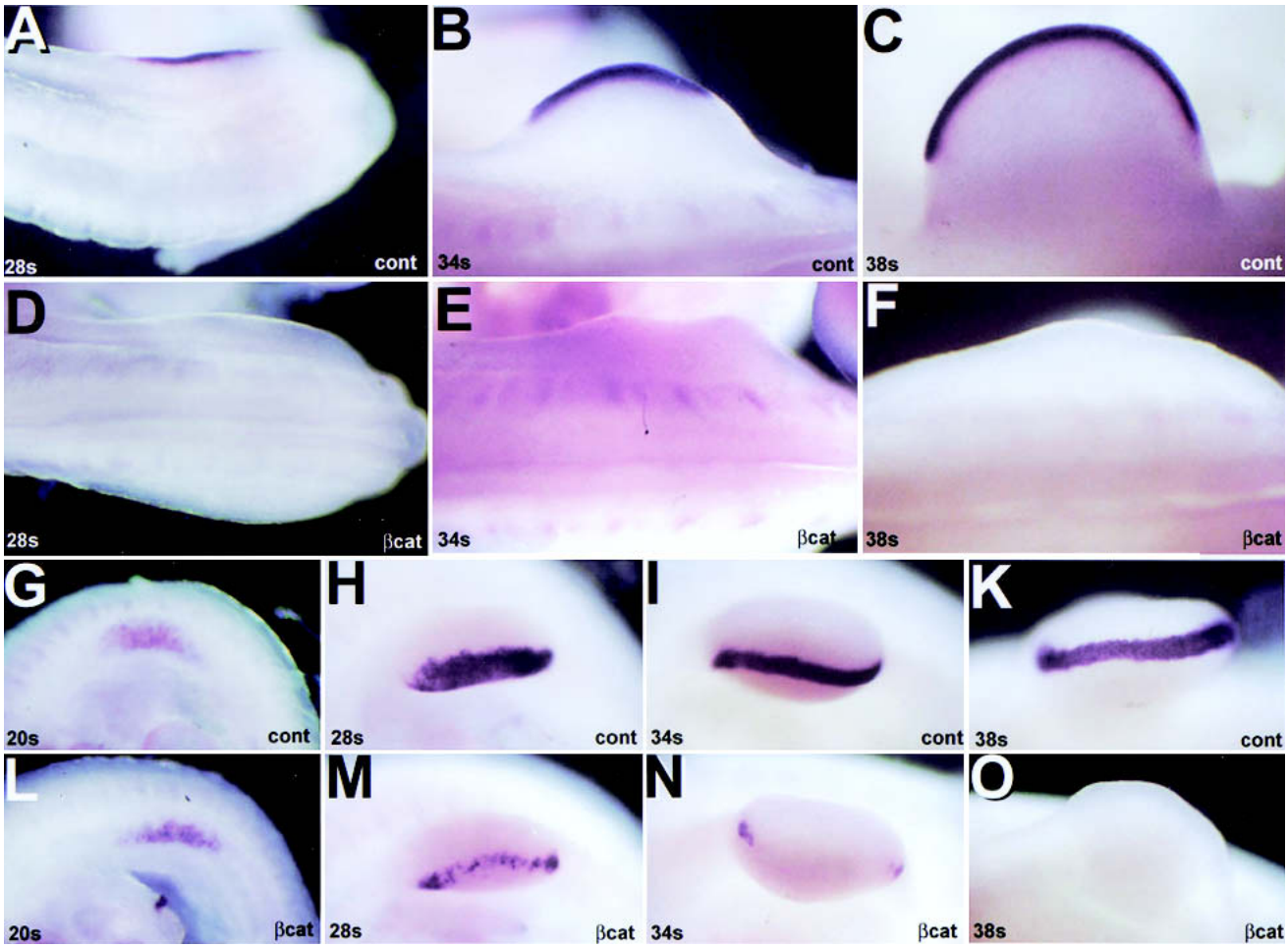

Figure 5. *Fgf8* expression is disrupted in the fore- and hindlimbs of β-*catenin*$^{n/c}$; *Msx2Cre* conditional mutants. (*A–F*) Dorsal views (anterior to the left) of control and mutant hindlimbs. *Fgf8* is never expressed at any stage of development in the hindlimb ectoderm of β-*catenin*$^{n/c}$; *Msx2Cre* mutants. (*G–O*) Distal views (anterior to the left) of control and mutant forelimbs. *Fgf8* expression initiates normally in the forelimb ventral ectoderm at 20 somites (*L*). It fades progressively at later stages (*M*,*N*) of development and is completely absent by 38 somites (*O*). cont, control; βcat, β-*catenin*; *Msx2Cre*; 20s, 28s, etc. refer to the age in somites of the embryo.

expressed throughout (data not shown). Interestingly, dorsoventral patterning in the forelimb initiated normally but the limbs became progressively dorsalized (data not shown). In severely affected *Wnt3*$^{n/c}$; *Msx2Cre* mutant hindlimbs, *En1* expression was absent, as was observed in mutants lacking β-*catenin* (data not shown). In mildly affected mutants, *En1* was expressed in the ventral ectoderm; however, no expression was observed in remnants of the AER (data not shown).

Cell death and cell proliferation in the ectoderm and mesenchyme of the developing limb in the absence of Wnt3/β-catenin *signaling*

Removal of the AER by surgical means initiates an immediate apoptotic effect in the distal limb mesenchyme of both the chick and mouse (Rowe et al. 1982; Dudley et al. 2002; Sun et al. 2002). This distal apoptosis may explain the distal truncations observed in the limb following AER removal (Dudley et al. 2002). To determine whether AER removal by genetic means would have similar consequences, we examined the levels of apoptosis in the *Wnt3* and β-*catenin* conditional mutant limbs. In normal embryos at early stages, no apoptosis was observed in the limb bud ectoderm or mesenchyme (Fig. 8A). However, after formation of the AER, elevated levels of apoptosis were detected in the thickened ectoderm of the AER through E11.5 (Fig. 8D,G,I,K,M) as reported elsewhere (Sun et al. 2002). Increased apoptosis was also observed in the dorsal proximal mesenchyme of wild-type embryos in the forelimbs and hindlimbs commencing at 35 somites and 38 somites, respectively (data not shown) in agreement with the findings of Sun et al. (2002). In *Wnt3* conditional mutant hindlimbs, no significant apoptosis was detected until the 35-somite stage (Fig. 8B,E) when apoptosis was apparent throughout the mesenchyme and ectoderm. Apoptosis continued through to 42 somites (E11.25) but could not be detected at E11.5 (data not shown). The elevated mesenchymal apoptosis was generally more significant dorsally. No ectopic apoptosis was observed in the forelimbs (data not shown).

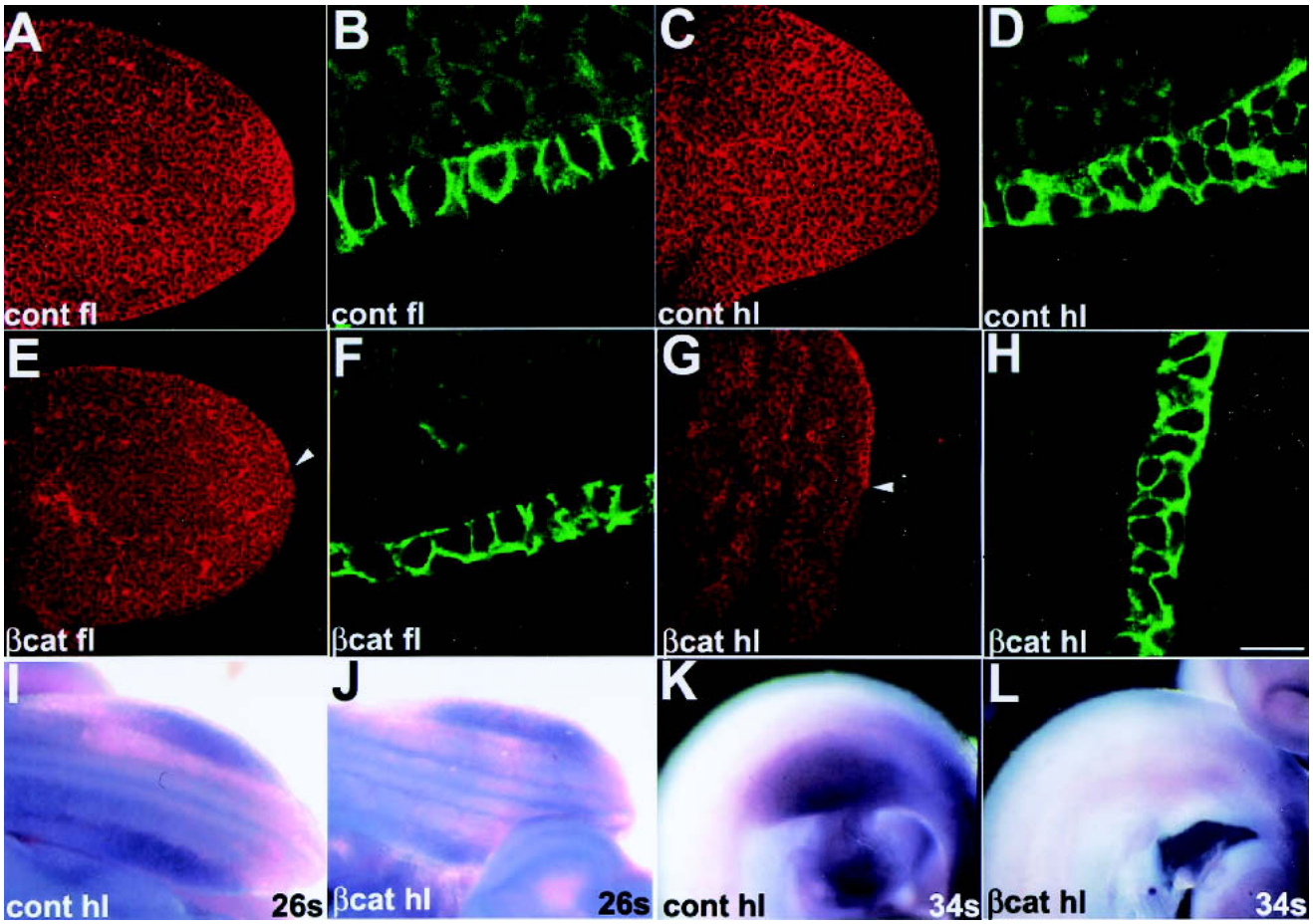

Figure 6. β-*catenin* removal in the limb ectoderm does not affect cell adhesion in the limb ectoderm nor induction of *Fgf10* in the mesenchyme. (*A–H*) Transverse sections (dorsal side up) through the fore- and hindlimbs of control and mutant embryos at 35 somites stained with β-catenin (rhodamine), and high-magnification views of ventral ectoderm from neighboring sections stained with E-cadherin (FITC) antibodies. In the control embryos (*A–D*), both β-catenin and E-cadherin antibodies stain the membranes throughout the limb ectoderm. In the β-*catenin*; *Msx2Cre* mutants, however, β-*catenin* protein is restricted to the dorsal ectoderm (arrowheads, *E*,*G*). (*F*,*H*) Despite the absence of β-catenin in the ventral ectoderm, E-cadherin remains properly localized to the membranes of ventral ectodermal cells. Views of embryonic limb buds subjected to *Fgf10* in situ hybridization. Note that early β-*catenin*$^{n/c}$; *Msx2Cre* mutants exhibit normal *Fgf10* expression (*I*,*J*), whereas at later stages *Fgf10* is not maintained (*K*,*L*); arrows denote the position of the hindlimb. cont, control; βcat, β-*catenin*; *Msx2Cre*; Bar: *A*,*C*,*E*,*G*, 100 μm; *B*,*D*,*F*,*H*, 25 μm.

In β-*catenin* mutants, we detected elevated cell death in the ectoderm of the hindlimb but not in the associated mesenchyme at 29 somites (Fig. 8C). By 35 somites, we observed massive apoptosis throughout the ectoderm and mesenchyme of the hindlimb (Fig. 8F), similar to that observed in *Wnt3* conditional mutants. In the forelimb of the β-*catenin*; *Msx2Cre* mutants, apoptosis was elevated in the distal mesenchyme and ectoderm (Fig. 8J). At 38 somites, apoptosis was extensive throughout the mesenchyme and ectoderm of the hindlimb buds (data not shown), whereas in the forelimb cell death was again restricted to the distal ectoderm and mesenchyme (Fig. 8L). By E11.5, apoptosis in the limb ectoderm and mesenchyme in both the fore- and hindlimb had ceased (Fig. 8N; data not shown). In summary, these results suggest that AER activity is required for survival of both the mesenchyme and ectoderm of the limb. In contrast to the surgical ablation studies, where the apoptotic effect in the mesenchyme is immediate (Rowe et al. 1982; Dudley et al. 2002; Sun et al. 2002), we observed a delay in apoptosis in the mesenchyme. We also found that there is a difference in the extent and location of apoptosis depending on the time that the AER is removed. In the case of the β-*catenin* mutant hindlimbs, where an AER never forms, apoptosis is extensive throughout the mesenchyme (and ectoderm) of the limb. In the forelimb, however, where the AER disappears later in development, apoptosis is restricted to the distal mesenchyme (and ectoderm).

In contrast to the increased cell death in the absence of *Wnt3*/β-*catenin* signaling, examination of cell proliferation failed to demonstrate any consistent reduction in the phosphohistone H3 labeling index in the mesenchyme or ectoderm of either mutant combination (see Supplementary Table 1).

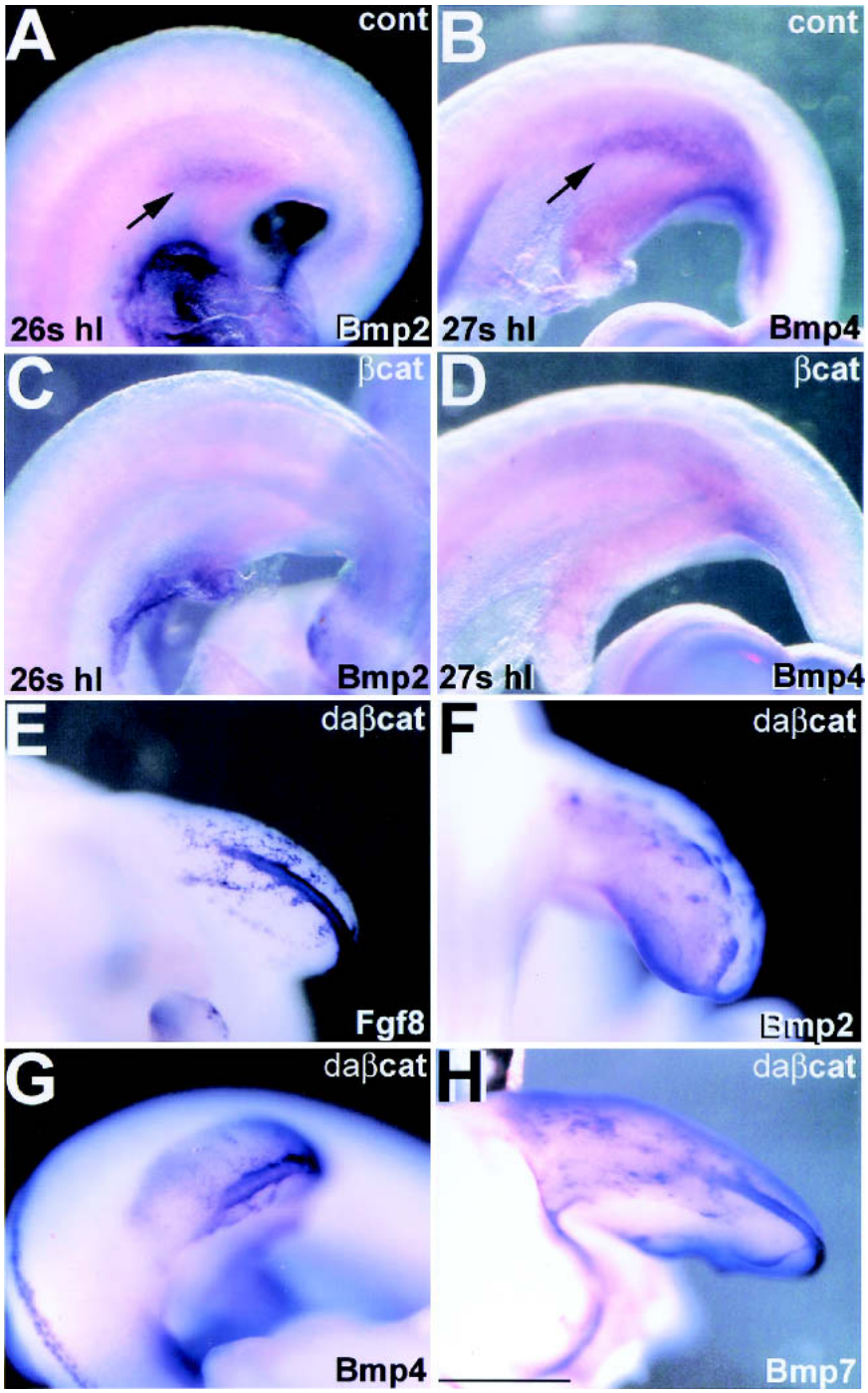

Figure 7. Ectodermal *Wnt*/β-*catenin* signaling lies upstream of *Bmp* signaling and dorsoventral patterning. Early expression of *Bmp2* (*A*,*C*) and *Bmp4* (*B*,*D*) in the ventral ectoderm (arrows, *A*,*B*) of the hindlimb is completely abolished in β-*catenin*$^{n/c}$; *Msx2Cre* mutants (*B*,*D*). Activation of β-*catenin* in the chick limb ectoderm induces the expression of *Fgf8* (*E*), *Bmp2* (*F*), *Bmp4* (*G*), and *Bmp7* (*H*) in both the dorsal and ventral ectoderm. cont, control; βcat, β-*catenin*; *Msx2Cre*; daβcat, dominant active β-*catenin*; 26s, 27s, etc. refer to the age in somites of the embryos. Bar, 300 μm.

Discussion

We have used *Wnt3* and β-*catenin* conditional mutants to address the role of *Wnt3*/β-*catenin* signaling in AER-mediated outgrowth of the limb. These studies indicate that *Wnt3*/β-*catenin* signaling is essential for the establishment and the maintenance of the AER. In addition, they suggest that although *Wnt3* is expressed throughout the ectoderm of the limb, the ventral ectodermal cells of the pre-AER appear to be the only population competent to respond to the *Wnt3* signal. Finally, our studies demonstrate that *Wnt3*/β-*catenin* signaling is required for the expression of the ventral ectodermally expressed *Bmp2* and *Bmp4*, which are important in the establishment of correct dorsoventral pattern within of the limb field, an apparent prerequisite for establishing the AER.

A Wnt3/β-catenin/Fgf *regulatory loop in AER establishment and maintenance*

The temporal kinetics of the *Msx2Cre* transgene in the fore- and hindlimbs demonstrate two distinct roles for

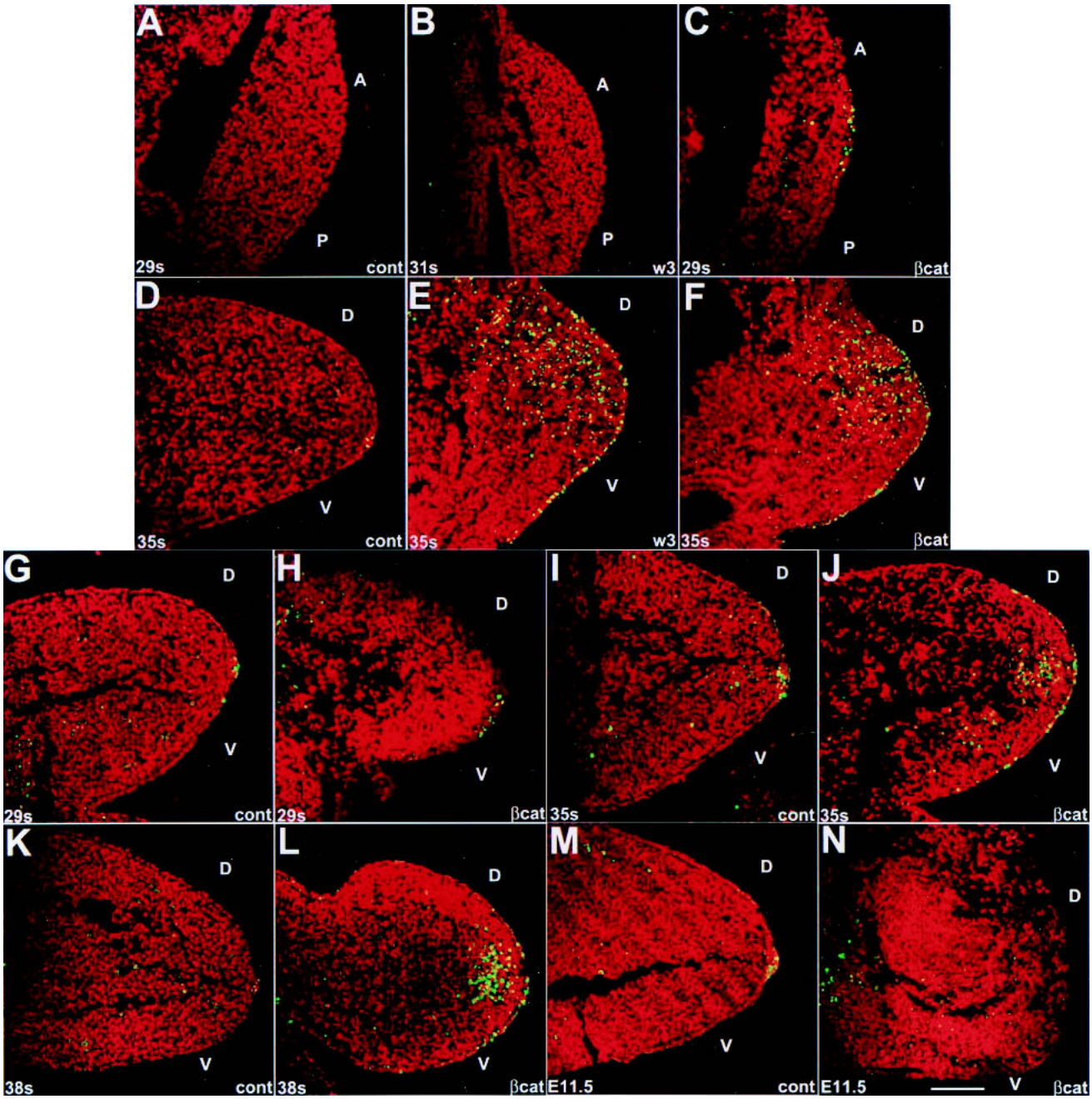

Figure 8. Lack of *Wnt*/β-*catenin* signaling in the limb ectoderm results in abnormal apoptosis in the ectoderm and mesenchyme of the limb. (*A–C*) Apoptosis in the hindlimbs of control and mutants at 29–30 somites. There is no apoptosis in the limb mesenchyme of the control, *Wnt3*, or β-*catenin* mutants. There is, however, apoptosis in the ectoderm of the β-*catenin* mutants. (*D–F*) At 35 somites (approximately a half-day after the induction of *Fgf8*), there is apoptosis in the AER of control embryos (*D*). In the *Wnt3* and β-*catenin* conditional mutants, there is extensive apoptosis throughout the limb mesenchyme and adjacent ectoderm. The apoptosis in the mesenchyme is more significant dorsally. (*G–N*) Apoptosis in the forelimbs of β-*catenin*$^{n/c}$; *Msx2Cre* mutants. At 29 somites, there is apoptosis in the AER of controls (*G*) and in the AER-like thickened ectoderm of the β-*catenin* mutants (*H*). There is, however, no apoptosis in the limb mesenchyme. (*J*,*L*) At 35–38 somites, there is extensive apoptosis in the distal mesenchyme and associated ectoderm. (*N*) By E11.5 no ectopic apoptosis can be observed. 29s, 34s, etc., refer to the age in somites of the embryo; A, anterior; cont, control, βcat, β-*catenin*; *Msx2Cre*; D, dorsal; P, posterior; V, ventral; w3, *Wnt3*; *Msx2Cre*. Bar, 100 μm.

β-catenin activity in establishment and maintenance of the AER. β-*catenin* is essential for the initiation of AER formation, as evidenced by the absence of any AER thickening or AER markers (*Bmp2*, *Bmp4*, *En1*, *Msx2*, *Fgf4*, *Fgf8*, *Wnt5a*) in the hindlimbs of β-*catenin*$^{n/c}$; *Msx2Cre* mutants. At forelimb levels, the failure to

maintain *Fgf8* expression following later removal of β-*catenin* activity indicates an ongoing role for β-*catenin* in maintenance of the AER. The failure of AER initiation and perhaps maintenance is phenocopied by removal of Wnt3 activity in the hindlimb ectoderm. Thus, our data provide strong support for the *Wnt*/β-*catenin*/*Fgf* regulatory loop proposed by Kawakami et al. (2001; see above), albeit that *Wnt3* and not *Wnt3a* is the key signal in the mouse. This model predicts that the removal of any one component of this regulatory loop would result in embryos that lack the AER and are consequently limbless. Supporting this view, embryos lacking *Fgf10*, *Wnt3*/β-*catenin*, or both *Fgf4* and *Fgf8* in their respective limb domains all result in complete loss of limbs. Another prediction is that removal of the ectodermal *Wnt3*/β-*catenin* or *Fgf* pathway should result in failure to maintain *Fgf10* expression in the mesenchyme. We and others have shown this to be the case (Fig. 6; Sun et al. 2002). Several observations, however, demonstrate that there is not a simple linear relationship between ectodermal *Wnt*/β-*catenin* signaling and *Fgf8*. First, in contrast to *Wnt*/β-*catenin* mutants which lack the AER, *Fgf8* single or *Fgf4/8* double mutants, which at least initially have no *Fgfs* expressed in the ridge, still possess an AER (Lewandoski et al. 2000; Moon and Capecchi 2000; Sun et al. 2002). In addition, genes expressed in the AER continue to be expressed in these *Fgf* mutants (Sun et al. 2002), whereas they are absent in the *Wnt3*/β-*catenin* mutants (data not shown). The consequences of these differences are perhaps most clearly manifested in comparison of the *Fgf4/8*; *Msx2Cre* (Sun et al. 2002) and the β-*catenin*; *Msx2Cre* (this study) mutant forelimbs. Although in both mutants the *Msx2Cre* activity would be predicted to remove *Fgf4/8* and β-*catenin* activities from their critical domains of function at the same time in development, the forelimb phenotype is dramatically different in each of the mutant backgrounds. In the *Fgf4/8* double mutant forelimbs, for example, remnants of each of the limb segments (i.e., stylopod, zeugopod, and autopod) remain, whereas the β-*catenin* mutants exhibit severe distal truncations at the level of the humerus. The basis for this phenotypic difference likely resides in the fact that in contrast to the β-*catenin* mutants, the *Fgf4/8* double mutants still possess an AER, and this AER is the source of two other Fgfs, Fgf9 and Fgf17 (Sun et al. 2002) that may have overlapping activities to Fgf4 and Fgf8. A second difference between the results reported here and those of the *Fgf4/8* double mutants is that low levels of Shh are maintained in the posterior distal mesenchyme of *Fgf4/8* double mutant forelimbs but not in those of β-*catenin* mutants. Thus, together Shh, Fgf9, and Fgf17 are likely sufficient to permit the formation of distal structures in the forelimbs of *Fgf4/8*; *Msx2Cre* mutants. Indeed, the dual presence of Fgf and Shh has been shown to correlate with the respecification of distal structures in chick limb regeneration models (Kostakopoulou et al. 1996; A. Dudley and C. Tabin, unpubl.). There are also quite distinct differences in the pattern of cell death following the removal of Fgf4/8 signaling and β-catenin activity. The *Fgf4/8* double mutants exhibit elevated apoptosis in the dorsal, proximal mesenchyme, whereas apoptosis is dramatically enhanced in the distal mesenchyme of β-*catenin* mutants, precisely the region of the limb bud that gives rise to more distal structures. As the AER plays an important role in survival of the limb mesenchyme cells (Dudley et al. 2002; Sun et al. 2002; this work), the basis for the differences is most likely due to the presence of the AER and the molecules expressed therein. In summary, *Wnt3*/β-*catenin* signaling appears to be doing more than simply inducing expression of ectodermal Fgfs. Indeed, one additional function appears to be the activation of other signaling pathways such as the *Bmp* signaling cascade en route to formation of the AER. Although the ectodermally expressed Fgfs are not critical for the formation of the AER, they may be critical for the maintenance of this structure. *Fgf4/8* double mutant hindlimbs exhibit a precocious loss of the AER (Sun et al. 2002), which may reflect a failure of the maintenance of mesenchymally derived *Fgf10* in these mutants. In addition to maintaining the *Wnt*/β-*catenin*/*Fgf* regulatory loop, the ectodermal Fgf signaling molecules are required for the activation/repression of many mesenchymal genes that are clearly important for limb outgrowth (i.e., the mesenchymal expression of *Bmp2*, *Bmp4*, *Msx1*, *Spry1*, *Spry2*, *Shh*, and repression of *Meis1* in the distal mesenchyme; Sun et al. 2002).

The establishment of the AER in the mouse and chick

The establishment of the AER appears to be regulated by the same signaling pathways in mouse and chick. In the chick, one of the first critical steps is the activation of *Fgf10* by *Wnt*/β-*catenin* signaling in the lateral plate mesenchyme at the level of the limb (Kawakami et al. 2001). It is possible that *Wnt*/β-*catenin* activation of *Fgf10* also occurs in the mouse. For example, simultaneous removal of *Lef1* and *Tcf1*, which likely eliminates canonical Wnt signaling in the mesenchyme as well as the ectoderm results in abrogation of the AER (Galceran et al. 1999). It remains to be seen whether *Fgf10* is expressed in the limb mesenchyme of these double mutants prior to AER induction. In the chick, *Fgf10*, once activated in the limb mesenchyme, appears to signal to the overlying ectoderm, triggering expression of *Wnt3a* (Kawakami et al. 2001); by analogy, *Wnt3* would be the mouse target. In the chick, *Wnt3a* expression is quickly restricted to the dorsoventral interface or to cells that will give rise to the AER. It appears that this restriction is important, as ectopic expression of *Wnt3a* in the non-AER ectoderm induces *Fgf8* expression and the formation of ectopic thickened ectoderm outside of the AER (Kengaku et al. 1998). It is important to note, however, that in the chick at least three other *Wnts*, *Wnt3*, *Wnt5a*, and *Wnt6*, are expressed more broadly in the chick limb ectoderm (Kengaku et al. 1997; C. Tabin and A. McMahon, unpubl.). Either these molecules have different signaling activities or some mechanism may be required to prevent Wnt signaling outside the AER (see below). In the mouse, however, *Wnt3* expression is never restricted to the AER, yet the *Msx2Cre*-mediated removal of

β-*catenin* activity suggests that reception of the apparently ubiquitous *Wnt3* signal is only effective in the ventral ectoderm, as these mutants possess normal β-*catenin* throughout most of the dorsal ectoderm yet lack an AER. Further evidence of restricted *Wnt3*/β-*catenin* signaling in the limb comes from transgenic embryos harboring a reporter construct activated by β-*catenin*-dependent transcription. In these embryos, activity is only observed within the AER (S. Piccolo, pers. comm.). How the Wnt3 signal is localized to the pre-AER/AER is not clear. It is possible that a molecule required to transduce canonical Wnt signals (i.e., a Frizzled receptor) is localized exclusively to the pre-AER (AER). Alternatively, it is conceivable that a repressor of *Wnt* signaling exists dorsally but is not present ventrally. The observation that Wnt3 ligand derived from the dorsal ectoderm is capable of signaling to the AER of *Wnt3* conditional mutant limbs argues against the possible antagonistic action of secreted factors such as frizzled-related proteins (sFRPs), which function by titrating secreted Wnt ligands (Leyns et al. 1997; Wang et al. 1997). Interestingly, naked cuticle 1 (Nkd1), which acts to inhibit the *Wnt*/β-*catenin* pathway at the level of dishevelled, exhibits a dorsal expression bias in the limb ectoderm (Wharton et al. 2001). Furthermore, removal of another Wnt antagonist, Dickkopf1 (Dkk1), results in an expanded AER (Mukhopadhyay et al. 2001). *Dkk1*, however, is expressed within the cells of the AER, suggesting that its role is not to restrict *Wnt3* signaling to the AER but perhaps to attenuate *Wnt3* signaling within the responding tissue.

Establishment of dorsoventral patterning in the mouse limb

Previous work has shown that the establishment of the AER is dependent on the establishment of dorsoventral polarity in the limb ectoderm (for review, see Chen and Johnson 1999). Our present results have shed light on that process. We have shown that mutants lacking *Wnt*/β-*catenin* signaling in the limb ectoderm also lack expression of ventrally expressed *Bmp* ligands. Furthermore, a dominant active form of β-catenin (daβ-catenin) activates these same ligands in the limb ectoderm of the chick. Thus, the *Wnt*/β-*catenin* pathway lies upstream of *Bmp* signaling in the limb ectoderm. Further, *En1* is not expressed in the ventral ectoderm, and the ventral mesenchyme of β-*catenin* mutants is dorsalized. These results support a model in which *Bmp* signaling is required for the establishment of *En1* expression in the ventral ectoderm, which then restricts expression of *Wnt7a* to the dorsal ectoderm and Wnt7a-dependent activation of *Lmx1b* to the dorsal mesenchyme (Riddle et al. 1995; Loomis et al. 1996, 1998; Ahn et al. 2001; Pizette et al. 2001). The loss of *Bmp* signaling has been reported to result in a failure in AER induction and *Fgf8* expression, similar to the *Wnt3*/β-*catenin* mutants (Ahn et al. 2001; Pizette et al. 2001). Hence, it would appear that *Bmp* signaling lies between the *Wnt*/β-*catenin* pathway and the induction of *Fgf8*. Several observations, however, seem to be in disagreement with this hypothesis. For example, our results in the chick demonstrated that *Fgf8* is strongly activated by daβ-*catenin* (94% of infected limbs), whereas activation of *Bmp* ligands was much less effective (20% of infected limbs), suggesting that β-catenin-mediated activation of *Fgf8* can occur in the absence of Bmp induction. Furthermore, Pizette et al. (2001) demonstrated that ectopic activation of *Bmp* signaling throughout the chick limb ectoderm only induces *Fgf8* expression in the dorsal ectoderm, suggesting that *Bmp* signaling is only indirectly responsible for inducing *Fgf8*. For example, *Bmp* signals in the dorsal ectoderm may create de novo dorsoventral interfaces that form ectopic AERs and are thus capable of expressing *Fgf8*. Further investigation will be required to determine the relationship between *Wnt3* and *Bmp* signaling in the activation/maintenance of *Fgf8*.

Our results provide strong genetic evidence that *Wnt3*/β-*catenin* signaling is required in the ectoderm to establish and maintain the presence of the AER in the mouse. In addition, our results show that *Wnt*/β-*catenin* signaling lies upstream of the ventrally expressed *Bmp* ligands as well as *Fgf8* and other genes expressed in the AER. It will be interesting to elucidate the mechanistic details whereby *Wnt*/β-*catenin* regulates these pathways and then to determine why coordinate expression of these pathways is critical for formation and function of the AER.

Materials and methods

Targeted mutagenesis of the Wnt3 *locus*

The *Wnt3* null ($Wnt3^n$) and conditional ($Wnt3^c$) alleles were introduced separately by homologous recombination into the genome of mouse embryonic stem (ES) cells. Both alleles were generated from a 9.5-kb fragment of genomic DNA extending from intron 1 to a *Bam*HI restriction endonuclease site at the 5′ end of exon 5 (Supplementary Fig. 1A). $Wnt3^n$ contains a neo^r gene (the pMC1neo cassette) inserted into a *Cla*I site in exon 4, generating a loss-of-function allele (Supplementary Fig. 1C). $Wnt3^c$ contains two *lox*P sites, inserted as double-stranded oligonucleotides, into the single *Not*I site in intron 2 and into the *Asp*718 site in intron 4 (Supplementary Fig. 1D). The 5′-most site was linked with a diagnostic *Bam*HI restriction-endonuclease site; the latter 3′ site had the insertion of an FRT-flanked neo^r cassette driven by mouse RNA polymerase II large subunit gene (data not shown). Genomic sequences containing the two alleles, $Wnt3^n$ and $Wnt3^c$, were then linked to the negative selectable HSV-TK gene and introduced into ES cells lines CC1.2 ($Wnt3^n$) or R1 ($Wnt3^c$). Following positive-negative selection (Mansour et al. 1988), selected clones were digested with *Eco*R1 and subjected to Southern blot analysis, where they were probed with a 3′ flanking probe that identifies a 23-kb fragment at the wild-type *Wnt3* genomic locus. The presence of an additional *Eco*RI site in the neo^r cassette in either mutant allele, however, generates a novel fragment length of either 9.8 kb ($Wnt3^n$; Supplementary Fig. 1F) or 9.2 kb ($Wnt3^c$; Supplementary Fig. 1G). The presence of the 5′-most *lox*P site in the $Wnt3^c$ allele was verified by identification of an additional *Bam*HI site following Southern transfer analysis of genomic DNA. ES cell lines harboring the appropriate $Wnt3^n$ or $Wnt3^c$ were injected into blastocysts and transferred to the germline of the resulting

chimeric founders. The FRT-flanked neo^r cassette in the *Wnt3^c* was removed by mating carrier animals with animals expressing the *FLPe* gene.

Genotyping of mice and embryos

Small pieces of ear from mice or yolk sacs from embryos were put in 100 µL of PCR lysis buffer (50 mM KCl, 10 mM Tris-Cl at pH 8.3, 2.5 mM $MgCl_2$, 0.1 mg/mL gelatin, 0.45% NP-40, 0.45% Tween 20) and 3 µL 20 mg/mL proteinase K at 50°C overnight. The samples were boiled for ~5 min, and then 1 µL was used for PCR analysis. For *Wnt3^n* genotyping, the primer set was *Wnt3* exon 4 sense: 5′-TGGCATTTCTCCTTCCGTTTCTC-3′, *Wnt3* exon 4 antisense: 5′-TGGTGGAGAAACACCGTGAGTC-3′, Neo sense: 5′-GCCTGCTTGCCGAATATCATGG-3′. The amplified wild-type band (i.e., the *Wnt3* exon 4 sense and antisense amplification product) was 258 bp, whereas the mutant band (neo sense and exon 4 antisense amplification product) was 350 bp. For the conditional allele, we used intron 4 sense: 5′-TTCTTAGATGGGCTTGTGATGTC-3′, intron 4 antisense: 5′-TGGCTTCAGCATCTGTTACCTTC-3′. The intron 4 amplification product was 230 bp for wild-type and 370 bp for *Wnt3^c*. The PCR primer sets described by Brault et al. (2001) were used for genotyping the β-*catenin* null and conditional alleles. PCR conditions for all primer sets were 95°C for 30 sec, 59°C for 20 sec, 72°C for 1 min repeated 34 times. The 35 cycles were followed by a 7-min extension step at 72°C. PCR products were resolved on 2% agarose gels.

Intercrosses to generate mutant embryos

Mice homozygous for the *Wnt3^c* allele are viable, fertile, and appear to be phenotypically normal. To determine the effect of limb-specific removal of the *Wnt3* gene, homozygous, *Wnt3$^{c/c}$* females were bred to males heterozygous for the *Wnt3* null allele, *Wnt3^n* (see Supplementary Fig. 1) and carriers of one of the two limb-specific Cre transgenes. Only embryos or mice that were *Wnt3$^{c/n}$*, and carriers of either the *Msx2* or *RARCre* transgene demonstrated any phenotypic abnormalities. All other allelic combinations resulted in normal appearance and served as controls. The same strategies were employed for the generation of β-*catenin$^{n/c}$*; *Msx2Cre* mutant embryos.

In situ hybridization and immunohistochemistry

^{35}S in situ hybridization was performed as described (Wilkinson et al. 1988).Whole mount digoxigenin in situ hybridization was carried out as described by Wilkinson and Nieto (1993). For immunohistochemistry, paraffin sections were dewaxed in xylenes and rehydrated. They were then subjected to antigen retrieval, where the sections were microwaved for 15 min in 1 mM Tris HCl (pH 8), 5 mM EDTA. They were then cooled on ice to room temperature. All incubations were done at room temperature. Slides were blocked for 30 min in 10% fetal bovine serum (FBS) in phosphate-buffered saline (PBS), 0.1% TritonX-100 (PBST), then incubated 1 h with primary antibodies (E-cadherin, Boussadia et al. 2002; β-*catenin*, Sigma) diluted 1:500 in PBST. The slides were then washed three times in PBST and then incubated for 1 h with fluorescently tagged secondary antibodies (Molecular Probes) diluted 1:500 in PBST.

Skeletal preparations, β-gal reporter analyses, and histology

Skeletal preparations were prepared as described by Chisaka et al. (1992). For Xgal treatment of embryos, *R26R/Msx2Cre* or *R26R/RARCre* double transgenic embryos were fixed, rinsed in PBS and incubated in Xgal as described (Whiting et al. 1991). For histological sections, embryos or tissues were fixed overnight at 4°C and then were dehydrated in a methanol series and embedded in paraffin. The embedded embryos were sectioned at a thickness of 6 µm.

Apoptosis and cell proliferation assays

For both the apoptosis and cell proliferation assays, we selected *Wnt3$^{n/c}$; Msx2Cre* mutants with severe hindlimb defects to minimize the effects of variable expressivity of this background. For mutants at 31 somites and younger, where the severity of the phenotype was not immediately apparent, we examined four mutant limb buds. Apoptosis assays were performed using the Apoptag® kit (Invitrogen) according to the manufacturer's specifications, counterstained in DAPI, and mounted in Vectashield mounting medium (Vector Laboratories). The proliferation assays were performed exactly as described by Yu et al. (2002). We took sections (2–18 sections per limb) that had been subjected to immunohistochemistry with antibodies to phosphohistone H3 (Upstate Biotechnology) and counterstained with DAPI. Two limbs for each age and genotype (specified in Supplementary Table 1) were counted. Using confocal microscopy, we counted phosphohistone H3-positive cells in the mesenchyme in a 2.3×10^4 µm^2 area immediately adjacent to the AER in controls and the corresponding area in the mutants.

Viral injections into chick limbs

Dominant active β-*catenin*-containing replication competent viruses were injected in the fore- and hindlimb primordial at stages 10–12 and then harvested at stages 22–24, as described (Kengaku et al. 1998).

Acknowledgments

We thank Brian Harfe and Cliff Tabin for injections of the daβ-*catenin* into chick embryos, and Cliff Tabin for helpful discussions concerning the data and sharing of unpublished results. We also thank Gail Martin for the provision of *Msx2Cre* transgenic mice as well as helpful discussions and sharing unpublished data. We thank Anne Boulet for histological preparations of the *RARCre*; R26R embryos. This work was supported by an NRSA postdoctoral fellowship (F32 HD08479) to J.R.B., and grants from the NIH to A.P.M. (DK56246, HD03249, NS 33642) and M.R.C.

The publication costs of this article were defrayed in part by payment of page charges. This article must therefore be hereby marked "advertisement" in accordance with 18 USC section 1734 solely to indicate this fact.

References

Aberle, H., Schwartz, H., and Kemler, R. 1996. Cadherin–catenin complex: Protein interactions and their implications for cadherin function. *J. Cell Biochem.* **61:** 514–523.

Ahn, K., Mishina, Y., Hanks, M.C., Behringer, R.R., and Crenshaw III, E.B. 2001. BMPR-IA signaling is required for the formation of the apical ectodermal ridge and dorsal-ventral patterning of the limb. *Development* **128:** 4449–4461.

Behrens, J., von Kries, J.P., Kuhl, M., Bruhn, L., Wedlich, D., Grosschedl, R., and Birchmeier, W. 1996. Functional interaction of β-catenin with the transcription factor LEF-1. *Nature* **382:** 638–642.

Bell, S.M., Schreiner, C.M., and Scott, W.J. 1998. The loss of

ventral ectoderm identity correlates with the inability to form an AER in the legless hindlimb bud. *Mech. Dev.* **74:** 41–50.

Boussadia, O., Kutsch, S., Hierholzer, A., Delmas, V., and Kemler, R. 2002. E-cadherin is a survival factor for the lactating mouse mammary gland. *Mech. Dev.* **115:** 53–62.

Brault, V., Moore, R., Kutsch, S., Ishibashi, M., Rowitch, D.H., McMahon, A.P., Sommer, L., Boussadia, O., and Kemler, R. 2001. Inactivation of the β-catenin gene by Wnt1-Cre-mediated deletion results in dramatic brain malformation and failure of craniofacial development. *Development* **128:** 1253–1264.

Chen, H. and Johnson, R.L. 1999. Dorsoventral patterning of the vertebrate limb: A process governed by multiple events. *Cell Tissue Res.* **296:** 67–73.

Chisaka, O., Musci, T.S., and Capecchi, M.R. 1992. Developmental defects of the ear, cranial nerves and hindbrain resulting from targeted disruption of the mouse homeobox gene Hox-1.6. *Nature* **355:** 516–520.

Crossley, P.H. and Martin, G.R. 1995. The mouse Fgf8 gene encodes a family of polypeptides and is expressed in regions that direct outgrowth and patterning in the developing embryo. *Development* **121:** 439–451.

Dudley, A.T., Ros, M.A., and Tabin, C.J. 2002. A re-examination of proximodistal patterning during vertebrate limb development. *Nature* **418:** 539–544.

Galceran, J., Farinas, I., Depew, M.J., Clevers, H., and Grosschedl, R. 1999. Wnt3a$^{-/-}$-like phenotype and limb deficiency in Lef1$^{-/-}$Tcf1$^{-/-}$ mice. *Genes & Dev.* **13:** 709–717.

Haegel, H., Larue, L., Ohsugi, M., Fedorov, L., Herrenknecht, K., and Kemler, R. 1995. Lack of β-catenin affects mouse development at gastrulation. *Development* **121:** 3529–3537.

Kawakami, Y., Capdevila, J., Buscher, D., Itoh, T., Rodriguez Esteban, C., and Izpisua Belmonte, J.C. 2001. WNT signals control FGF-dependent limb initiation and AER induction in the chick embryo. *Cell* **104:** 891–900.

Kengaku, M., Twombly, V., and Tabin, C. 1997. Expression of Wnt and Frizzled genes during chick limb bud development. *Cold Spring Harb. Symp. Quant. Biol.* **62:** 421–429.

Kengaku, M., Capdevila, J., Rodriguez-Esteban, C., De La Pena, J., Johnson, R.L., Belmonte, J.C., and Tabin, C.J. 1998. Distinct WNT pathways regulating AER formation and dorsoventral polarity in the chick limb bud. *Science* **280:** 1274–1277.

Kostakopoulou, K., Vogel, A., Brickell, P., and Tickle, C. 1996. 'Regeneration' of wing bud stumps of chick embryos and reactivation of Msx-1 and Shh expression in response to FGF-4 and ridge signals. *Mech. Dev.* **55:** 119–131.

Lewandoski, M., Sun, X., and Martin, G.R. 2000. Fgf8 signalling from the AER is essential for normal limb development. *Nat. Genet.* **26:** 460–463.

Leyns, L., Bouwmeester, T., Kim, S.H., Piccolo, S., and De Robertis, E.M. 1997. Frzb-1 is a secreted antagonist of Wnt signaling expressed in the Spemann organizer. *Cell* **88:** 747–756.

Liu, P., Wakamiya, M., Shea, M.J., Albrecht, U., Behringer, R.R., and Bradley, A. 1999. Requirement for Wnt3 in vertebrate axis formation. *Nat. Genet.* **22:** 361–365.

Loomis, C.A., Harris, E., Michaud, J., Wurst, W., Hanks, M., and Joyner, A.L. 1996. The mouse Engrailed-1 gene and ventral limb patterning. *Nature* **382:** 360–363.

Loomis, C.A., Kimmel, R.A., Tong, C.X., Michaud, J., and Joyner, A.L. 1998. Analysis of the genetic pathway leading to formation of ectopic apical ectodermal ridges in mouse Engrailed-1 mutant limbs. *Development* **125:** 1137–1148.

Lyons, K.M., Pelton, R.W., and Hogan, B.L. 1990. Organogenesis and pattern formation in the mouse: RNA distribution patterns suggest a role for bone morphogenetic protein-2A (BMP-2A). *Development* **109:** 833–844.

Mansour, S.L., Thomas, K.R., and Capecchi, M.R. 1988. Disruption of the proto-oncogene int-2 in mouse embryo-derived stem cells: A general strategy for targeting mutations to nonselectable genes. *Nature* **336:** 348–352.

Martin, G.R. 1998. The roles of FGFs in the early development of vertebrate limbs. *Genes & Dev.* **12:** 1571–1586.

Min, H., Danilenko, D.M., Scully, S.A., Bolon, B., Ring, B.D., Tarpley, J.E., DeRose, M., and Simonet, W.S. 1998. Fgf-10 is required for both limb and lung development and exhibits striking functional similarity to Drosophila branchless. *Genes & Dev.* **12:** 3156–3161.

Molenaar, M., van de Wetering, M., Oosterwegel, M., Peterson-Maduro, J., Godsave, S., Korinek, V., Roose, J., Destree, O., and Clevers, H. 1996. XTcf-3 transcription factor mediates β-catenin-induced axis formation in *Xenopus* embryos. *Cell* **86:** 391–399.

Moon, A.M. and Capecchi, M.R. 2000. Fgf8 is required for outgrowth and patterning of the limbs. *Nat. Genet.* **26:** 455–459.

Moon, A.M., Boulet, A.M., and Capecchi, M.R. 2000. Normal limb development in conditional mutants of Fgf4. *Development* **127:** 989–996.

Mukhopadhyay, M., Shtrom, S., Rodriguez-Esteban, C., Chen, L., Tsukui, T., Gomer, L., Dorward, D.W., Glinka, A., Grinberg, A., Huang, S.P., et al. 2001. Dickkopf1 is required for embryonic head induction and limb morphogenesis in the mouse. *Dev. Cell* **1:** 423–434.

Pinson, K.I., Brennan, J., Monkley, S., Avery, B.J., and Skarnes, W.C. 2000. An LDL-receptor-related protein mediates Wnt signalling in mice. *Nature* **407:** 535–538.

Pizette, S., Abate-Shen, C., and Niswander, L. 2001. BMP controls proximodistal outgrowth, via induction of the apical ectodermal ridge, and dorsoventral patterning in the vertebrate limb. *Development* **128:** 4463–4474.

Riddle, R.D., Ensini, M., Nelson, C., Tsuchida, T., Jessell, T.M., and Tabin, C. 1995. Induction of the LIM homeobox gene Lmx1 by WNT7a establishes dorsoventral pattern in the vertebrate limb. *Cell* **83:** 631–640.

Roelink, H. and Nusse, R. 1991. Expression of two members of the Wnt family during mouse development—Restricted temporal and spatial patterns in the developing neural tube. *Genes & Dev.* **5:** 381–388.

Rowe, D.A., Cairns, J.M., and Fallon, J.F. 1982. Spatial and temporal patterns of cell death in limb bud mesoderm after apical ectodermal ridge removal. *Dev. Biol.* **93:** 83–91.

Saunders, J.W. 1948. The proximo-distal sequence of origin of the parts of the chick wing and the role of the ectoderm. *J. Exp. Zool.* **108:** 363–403.

Saxton, T.M., Ciruna, B.G., Holmyard, D., Kulkarni, S., Harpal, K., Rossant, J., and Pawson, T. 2000. The SH2 tyrosine phosphatase shp2 is required for mammalian limb development. *Nat. Genet.* **24:** 420–423.

Sekine, K., Ohuchi, H., Fujiwara, M., Yamasaki, M., Yoshizawa, T., Sato, T., Yagishita, N., Matsui, D., Koga, Y., Itoh, N., et al. 1999. Fgf10 is essential for limb and lung formation. *Nat. Genet.* **21:** 138–141.

Soriano, P. 1999. Generalized lacZ expression with the ROSA26 Cre reporter strain. *Nat. Genet.* **21:** 70–71.

Sun, X., Lewandoski, M., Meyers, E.N., Liu, Y.H., Maxson Jr., R.E., and Martin, G.R. 2000. Conditional inactivation of Fgf4 reveals complexity of signalling during limb bud development. *Nat. Genet.* **25:** 83–86.

Sun, X., Mariani, F.V., and Martin, G.R. 2002. Functions of FGF signalling from the apical ectodermal ridge in limb develop-

ment. *Nature* **418:** 501–508.
Takada, S., Stark, K.L., Shea, M.J., Vassileva, G., McMahon, J.A., and McMahon, A.P. 1994. Wnt-3a regulates somite and tailbud formation in the mouse embryo. *Genes & Dev.* **8:** 174–189.
Wang, S., Krinks, M., Lin, K., Luyten, F.P., and Moos Jr., M. 1997. Frzb, a secreted protein expressed in the Spemann organizer, binds and inhibits Wnt-8. *Cell* **88:** 757–766.
Wharton Jr., K.A., Zimmermann, G., Rousset, R., and Scott, M.P. 2001. Vertebrate proteins related to *Drosophila* Naked Cuticle bind Dishevelled and antagonize Wnt signaling. *Dev. Biol.* **234:** 93–106.
Whiting, J., Marshall, H., Cook, M., Krumlauf, R., Rigby, P.W., Stott, D., and Allemann, R.K. 1991. Multiple spatially specific enhancers are required to reconstruct the pattern of Hox-2.6 gene expression. *Genes & Dev.* **5:** 2048–2059.
Wilkinson, D.G. and Nieto, M.A. 1993. Detection of messenger RNA by in situ hybridization to tissue sections and whole mounts. *Methods Enzymol.* **225:** 361–373.
Wilkinson, D.G., Peters, G., Dickson, C., and McMahon, A.P. 1988. Expression of the FGF-related proto-oncogene int-2 during gastrulation and neurulation in the mouse. *EMBO J.* **7:** 691–695.
Yu, J., Carroll, T.J., and McMahon, A.P. 2002. Sonic hedgehog regulates proliferation and differentiation of mesenchymal cells in the mouse metanephric kidney. *Development* **129:** 5301–5312.